DIAGENETIC ALTERATION OF IRON(III) MINERALS TO HEMATITE AND IMPLICATIONS FOR THE VERA RUBIN RIDGE, MARS. A. L. Knight[1*], J. G. Catalano[1], and K. Mitra[1,2], [1]Department of Earth & Planetary Sciences, Washington University in St. Louis, St. Louis, MO 63130; [2]Department of Geosciences, Stony Brook University, Stony Brook, NY 11794; [*](alknight@wustl.edu).

Introduction: Hematite (α-Fe_2O_3) is the thermodynamically stable form of Fe(III) oxide and, given enough time, should form from precursor phases via diagenesis [1]. Particle size affects the color of hematite, with fine-grained (<3-5 μm) particles red and coarse-grained (>3-5 μm) particles gray [2]. Visible and near infrared (VNIR) spectroscopy can be used to distinguish red and gray hematite by their distinct spectral features, and both red and gray hematite have been identified in the Vera Rubin ridge (VRR) in Gale crater, Mars [3-4]. The VRR is a competent sedimentary ledge that is believed to have experienced several diagenetic episodes throughout its history [4-6]. At least one of these episodes likely produced the decameter-scale patches of gray hematite observed by the Mars Science Laboratory (MSL) *Curiosity* rover in the Jura member [3]. However, the nature of these fluids and the precursor mineralogy are not yet well-characterized.

Other iron (III) oxides are abundant on Mars and have been observed across the surface in the dust, soil, and regolith by both orbital and rover missions [7-10]. Iron (III) minerals, such as these, may be precursor minerals to the gray hematite observed at the VRR today. In addition to transformation from other Fe(III) oxides, hematite may coarsen to form larger, more stable particles with decreased surface area over time [11]. In this work, we have conducted a series of laboratory experiments to simulate the transformation of Fe(III) minerals in an array of diagenetic fluid conditions to identify potential formation pathways for the gray hematite observed at the VRR.

Methods: Initial minerals akaganeite (β-FeOOH), ferrihydrite ($Fe_{10}O_{14}OH$), goethite (α-FeOOH), red (~50 nm) hematite, nanophase (~10 nm) hematite, potassium jarosite ($KFe_3(SO_4)_2(OH)_6$), and schwertmannite ($Fe_{16}O_{16}(OH)_y(SO4)_z \cdot 7\ nH_2O$) were synthesized via standard laboratory techniques [12-15] and characterized via X-ray diffraction (XRD) using a Bruker d8 Advance powder X-ray diffractometer. Each mineral was suspended in a Mars-relevant [16] salt solution (either 1 M $MgCl_2$ or $MgSO_4$), for a total volume of 20 mL. Additional experiments to further investigate jarosite in 0.1 M salt solutions were performed as well. Each sample was set to an initial pH value of either 3 or 7 to simulate acidic and neutral conditions, respectively, and heated in a digital convection oven at either 98°C or 200°C. Samples raised to 98°C were sealed in test tubes lined with PTFE thread seal tape to reduce fluid evaporation. Samples heated to 200°C were sealed in PTFE-lined bombs (Parr Instrument Co.) required for hydrothermal conditions.

After 20 days, samples were removed from the convection oven and cooled to room temperature. The solid transformation products and fluids were separated via syringe filtration, using a 0.22 μm mixed cellulose ester (MCE) filter. The final pH values of the fluids were measured, and dissolved ion concentrations were determined with a Thermo iCap 7400 Duo ICP-OES via inductively-coupled plasma optical emission spectrometry (ICP-OES). The solid transformation products were washed with ultra-pure water, dried in a digital convection oven, ground with a mortar and pestle, and analyzed via powder XRD. Crystallite sizes and abundances of the solid products were determined using Profex to perform Rietveld refinement on the XRD patterns [17].

A Thermofisher Quattro S Scanning Electron Miscroscope (SEM) was used to characterize the particle size and morphology of select samples. All solid products were analyzed via VNIR spectroscopy with an Analytical Spectral Devices (ASD) portable VNIR spectroradiometer to distinguish red and gray hematite by their key absorption features and corroborate the final mineralogy of the samples.

Results: All initial minerals transformed to or remained hematite in at least some fluid conditions (Figure 1). Red hematite was generally the most common transformation product of the initial minerals investigated, but some samples transformed to goethite or remained untransformed. Neither red nor nanophase hematite coarsened substantially.

The only mineral that reacted to form gray hematite was jarosite. At elevated (200°C) temperatures, jarosite often at least partially converted to coarse-grained hematite, and when aged with fluids containing 1 M $MgCl_2$ at 200°C for 20 days, jarosite completely converted into coarse-grained crystals of gray hematite (Figure 2a). When subjected to the same conditions but with only 0.1 M $MgCl_2$ present in the fluid, jarosite only partially converted to gray hematite (Figures 1 and 2b).

Discussion: The final particle size of a mineral is controlled by its nucleation rate. Slow (but complete) dissolution of the precursor phases decreases the nucleation rate and increases the final particle size of the transformation product (e.g., hematite) [18]. Characterization of the fluid products of the jarosite

samples indicates that jarosite may be dissolving incongruently, as has been previously observed [19], which may promote a slow initial dissolution rate and the formation of larger final particles of hematite. The presence of chloride may also affect the transformation products of jarosite by promoting the removal of iron from the structure of jarosite [20]. Chloride, therefore, has an active role in completing the transformation of jarosite to hematite (Figure 2).

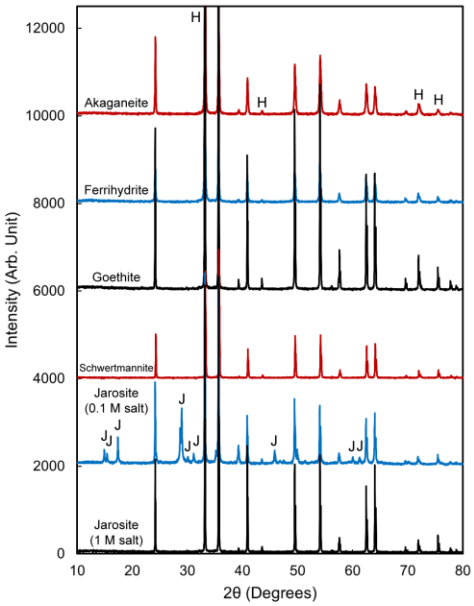

Figure 1: XRD patterns of the products of Fe(III) minerals subjected to Cl-rich, acidic (pH 3), 200°C fluids for 20 days. All initial minerals fully transformed to hematite (H) under these conditions except jarosite (J) in 0.1 M $MgCl_2$ fluids, which only partially transformed. Offset: 2000 (arb. unit).

Additional experiments investigating the dissolution and transformation of jarosite are needed to identify the geochemical mechanisms involved in the formation of gray hematite from jarosite and to quantify the time scales required for these processes to occur. Nevertheless, the results of this study suggest that jarosite transforming in acidic (particularly chloride-rich) fluids at elevated temperatures is a potential pathway to the gray hematite observed at the VRR. With increased aging and temperature, further coarsening of red and nanophase hematite may occur. However, the several orders of magnitude of grain growth required to generate gray hematite suggest this may not be a viable formation pathway. In contrast, the transformation of precursor Fe(III) minerals, such as jarosite, may offer a more rapid formation pathway for the gray hematite observed at the VRR. This is further supported by the presence of jarosite within the VRR, as observed by *Curiosity* [5].

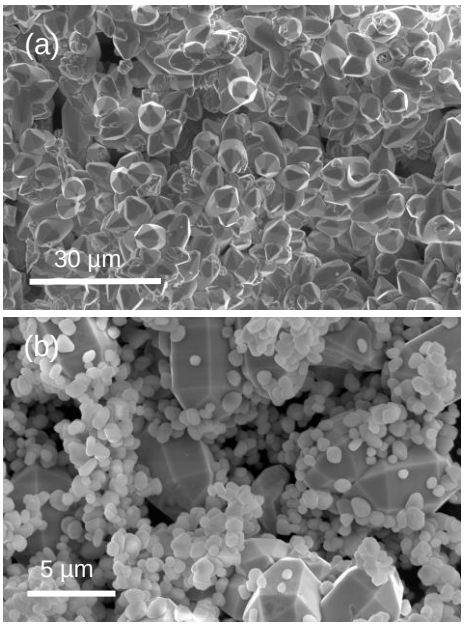

Figure 2: (a) SEM image of the transformation product (gray hematite) of jarosite when subjected to acidic (pH 3) fluids containing 1 M $MgCl_2$ at 200°C for 20 days. **(b)** SEM image of the transformation products of jarosite when subjected to acidic fluids containing 0.1 M $MgCl_2$ at 200°C for 20 days. Large gray hematite crystals with distinct faces are surrounded by smaller, rounded jarosite particles.

References: [1] Gooding J. L. (1978) *Icarus, 33*, 483–513. [2] Morris R. V. et al. (2000) *JGRP, 105*, 1757–1817. [3] Fraeman A. A. et al. (2020) *JGRP, 125*, e2019JE006294. [4] Horgan B. H. N. et al. (2020) *JGRP, 125*, e2019JE006322. [5] Rampe E. B. et al. (2020) *JGRP, 125*, e2019JE006306. [6] Thomas N. H. et al. (2020) *JGRP, 125*, e2019JE006289. [7] Morris R. V. et al. (2006) *JGRP, 111*, E12S15. [8] Bridges J. C. et al. (2001) *Space Sci. Rev., 96*, 365-392. [9] Grotzinger J. P. et al. (2015) *Science, 350*, aac7575. [10] McLennan S. M. et al. (2005) *EPSL, 240*, 95-131. [11] Walker T. R. et al. (1981) *JGR, 86*, 317-333. [12] Schwertmann U. and Cornell R. M. (2000) *Wiley and Sons.* [13] Madden A. S. and Hochella M. F. (2005) *Geochim. Cosmochim. Acta, 69*, 389-398. [14] Mulvaney P. et al. (1988) *Langmuir, 4*, 1206-1211. [15] Baron D. and Palmer C.D. (1996) *Geochim. Cosmochim. Acta, 60*, 185-195. [16] Newsom H. E. et al. (1999) *JGRP, 104*, 8717-8728. [17] Doebelin N. and Kleeberg R. (2015) *J. App. Cryst., 48*, 1573-1580. [18] Blesa M. A. and Matijević E. (1989) *Adv. Colloid Interface Sci., 29*, 173-221. [19] Smith A. M. L. et al. (2006) *Geochim. Cosmochim. Acta, 70*, 608–621. [20] Pritchett B. N. et al. (2012) *EPSL, 357-358*, 327-336.